

# Chapter One

## 1.1 Introduction :

Radiography has evolved over the years from using screen-film technology to digital imaging, which is sometimes referred to as filmless radiography. Nowadays, digital X-ray units are ubiquitous in most radiology departments [Marshall 2007].

Digital imaging is a term used to describe general radiography when the radiographic images are in digital form and are capable of being displayed on a computer monitor [Davidson 2006]. Digital imaging can be realized through the use of either computed radiography or digital radiography. It has become technically possible and economically feasible for digital imaging technologies to challenge screen-film technology for projection radiography [Gallet et.al 2009]. This has been made possible by the prerequisite technological advances such as high-luminance and high-resolution display monitors combined with high-performance computer workstations and a decline in the price of computer technology. This shift in choice of imaging modality is not only confined to developed countries but is gradually finding its way to developing countries.

Computed radiography uses an imaging plate coated with photostimulable phosphors to capture x-rays as they traverse through the patient. BaFBr:Eu<sup>2+</sup> and BaFI:Eu<sup>2+</sup> are the commonly used phosphors [Schaefer et.al 2009]. When exposed to radiation, the phosphors absorb and store x-ray energy in gaps of their altered crystal structure. This trapped energy comprises a latent image. When stimulated by additional light energy of the proper wavelength, the trapped energy is released. The amount of light emitted is directly proportional to the number of X-ray photons absorbed. The resulting computed radiography image comprises of multiple rows and columns of pixels representing the X-ray intensities at locations (x, y). Eventually, these raw pixel values are processed using mathematical algorithms for subsequent display.

In digital radiography, the digitization of the X-ray projection image occurs within the image receptor. Detectors in digital radiography can be in the form of charged coupled devices or flat panel imagers. Furthermore, flat panel imagers are generally of two types namely, direct conversion or indirect conversion systems. Direct conversion systems use an X-ray sensitive photoconductor layer (amorphous selenium, a-Se) and a thin-film transistor (TFT) [Schaefer et.al

2009]charge collector. Radiation absorbed by the photoconductor is directly converted into charge, which is drawn to the TFT charge collector where it is stored until readout. On the other hand, indirect conversion systems use scintillators e.g. cesium iodide (CsI) or gadolinium oxysulphide (Gd<sub>2</sub>O<sub>2</sub>S) layered on top of an array of light-sensitive photodiodes with TFTs. The scintillator converts radiation into light that is detected by the photodiode/TFT array. For anatomical regions with gross density differences such as the chest, thoracic spine, shoulder, facial bone, cervical spine, thoraco-lumbar spine, femur and feet, digital radiography has shown superior image quality over screen-film radiography [Davidson 2006].

## **1.2 Problem of study:**

Over the last few years, public hospitals in Khartoum state have been purchasing digital units for their radiology departments. This is in line with worldwide trends of migration from screen-film radiography to digital radiography. Upon adoption of new technology, it is advisable that the technology undergoes evaluation and critique so that strategies are devised to optimize its use. The transition from screen-film to digital radiography technology is not a simple matter, as it involves acquirement of new skills, change in the workflow process, training and retraining at times.

## **1.3 Objectives:**

### **1.3.1 General objective:**

- To estimate entrance skin dose for the patients from Digital Radiography x-ray.

### **1.3.2 Specific objectives:**

- To investigate the correlation between ESD and BMI, age, kVp and mAs.

## **1.4 Thesis layout:**

This study will contain five chapters, chapter one contains introduction and objectives of the study. Chapter two contains literature review, chapter three contains material and method, chapter four contains results and in chapter five there are discussion, conclusion and recommendations.

## **Chapter two**

### **2.1 Digital Radiography:**

Digital radiographic (DR) image receptors are gradually replacing screen-film cassettes as radiology departments convert to an all-digital environment. Computed tomography (CT) and magnetic resonance imaging (MRI) are intrinsically digital, and ultrasound and nuclear medicine imaging made the change to digital imaging from their analog ancestries in the 1970s [Bushberg et.al 2002]. Experimental digital subtraction angiography was first described in 1977 by Kruger et.al and introduced into clinical use as the first digital imaging system in 1980. For general radiography, x-ray images were first recorded digitally with cassette-based storage-phosphor image plates, which were also introduced in 1980. The first DR system, which appeared in 1990, was the CCD slot-scan system. In 1994, investigations of the selenium drum DR system were published. The first flat-panel detector DR systems based on amorphous silicon and amorphous selenium were introduced in 1995. Gadolinium-oxide sulfide scintillators were introduced in 1997 and have been used for portable flat-panel detectors since 2001 [Puig 2003]. The latest development in digital radiography is dynamic flat-panel detectors for digital fluoroscopy and angiography [Choquette et.al 2001].

The most obvious advantage of digital detectors is that they allow implementation of a fully digital picture archiving and communication system, with images stored digitally and available anytime. Thus, distribution of images in hospitals can be achieved electronically by means of web-based technology without the risk of losing images. Other advantages include higher patient throughput, increased dose efficiency, and the greater dynamic range of digital detectors with possible reduction of x-ray exposure to the patient.

The physical principles of digital radiography do not differ much from those of screen-film radiography. However, in contrast to screen-film radiography, in which the film serves as both detector and storage medium, digital detectors are used only to generate the digital image, which is then stored on a digital medium. Digital imaging comprises four separate steps: generation, processing, archiving, and presentation of the image.

The digital detector is exposed to x-rays generated by a standard tube. Ultimately, the energy absorbed by the detector must be transformed into electrical charges, which are then recorded, digitized, and quantified into a gray scale that represents the amount of x-ray energy deposited at each digitization locus in the resultant digital image. After sampling, post processing software is needed for organizing the raw data into a clinically meaningful image.

After final image generation, images are sent to a digitized storage archive. A digital header file containing patient demographic information is linked to each image. Although it is possible to print digital images as hard-copy film, the advantages of digital radiography are not realized completely unless images are viewed digitally on a computer workstation. Digital images can be manipulated during viewing with functions like panning, zooming, inverting the gray scale, measuring distance and angle, and windowing. Image distribution over local area networks is possible. Digital images and associated reports can be linked to a digital patient record for enhanced access to diagnostic data [Spahn 2005].

## **2.2 Digital Detectors:**

Digital radiography can be divided into CR and DR. CR systems use storage-phosphor image plates with a separate image readout process; DR is a way of converting x-rays into electrical charges by means of a direct readout process. DR systems can be further divided into direct and indirect conversion groups depending on the type of x-ray conversion used.

### **2.2.1 Computed radiography:**

Computed radiography (CR) is the most common method of producing digital radiographic images and the first technology that was commercially available [P. Allisy et.al 2008]. Is a marketing term for photostimulable phosphordetector (PSP) systems Phosphors used in screen-film radiography, such as Gd<sub>2</sub>O<sub>2</sub>S emit light promptly (virtually instantaneously) when struck by an x-ray beam. When x-rays are absorbed by photostimulable phosphors, some light is also promptly emitted, but much of the absorbed x-ray energy is trapped in the PSP screen and can be read out later. For this reason, PSP screens are also called storage phosphors or imaging plates. CR was introduced in the 1970s, saw increasing use in the late 1980s, and was in wide use at the turn of the century as many

departments installed PACS, often in concert with the development of the electronic medical record [Bushberg et.al 2002].

The phosphor in a powdered form is mixed with a binder or adhesive material and laid down on a base with a thickness of about 0.3mm. A surface coat protects the phosphor from physical damage. The imaging plate thus formed is similar in appearance to the intensifying screen used in conventional radiography. The plate is inserted into a light-tight cassette, also similar in appearance and with the same dimensions as that used for film-screen radiography. For this reason, X-ray equipment used for conventional radiography can be used for CR, making the transition from analogue to digital radiography straightforward [P. Allisy et.al 2008].

Radiographic films may be digitized after they are acquired with conventional film/screen systems. In a typical film digitizer, a laser beam is scanned across a film. The pattern of optical densities on the film modulates the transmitted light. A light detector on the opposite side of the film converts the transmitted laser light to an electrical signal that is digitized by an analog-to-digital converter. Spatial resolution of a film scanner is determined by spot size, defined as the size of the laser beam as it strikes the film. Spot sizes down to 50  $\mu\text{m}$  ( $50 \times 10^{-6}\text{ m}$ ) are available, but most clinical systems use 100  $\mu\text{m}$  or larger. Because the laser spot must be scanned across the entire area of the image, a decrease in the diameter of the spot size by a factor of 2 requires a scan time that is 4  $\times$  longer, if no other adjustments are made in the system. Commercially available laser film scanners have matrix sizes of at least  $2000 \times 2000 \times 10$  or 12 bits [Hendee et.al 2002].

The time for a CR reader to extract the image from the plate is generally between about 30 and 45s, and the faster readers are capable of reading 100 or more plates per hour. To achieve the fastest throughput, stacking readers are available in which several cassette (at least four) may be placed in a queue for automatic feed into the reader. Stacking readers are particularly useful for readers serving more than one X-ray room [P. Allisy et.al 2008].

One of the advantages of a stimulatable phosphor plate system over conventional film is an improvement in dynamic range. Radiographic film operates over possible exposures ranging from the exposure required to reach the shoulder of the characteristic curve to that required to rise above the toe. This range typically causes exposure differences of a factor of approximately 100. The dynamic range of a storage phosphor is on the order of 10,000. Thus

the storage phosphor has greater latitude (i.e., is more “forgiving”) if an incorrect exposure is used. To preserve the information contained within such a broad dynamic range, the analog-to-digital converter must have a sufficient bit depth a typical storage phosphor readout system is capable of digitizing a  $2000 \times 2000$  pixel matrix or greater, with each pixel taking one of  $2^{10} = 1024$  possible values. The images may then be processed according to a number of possible gray-scale mapping functions or simply windowed and levelled in a fashion similar to that used for magnetic resonance and CT images. Image processing techniques may also be used to enhance the appearance of edges of structures such as tubes in chest radiographs taken in intensive care units. Some of the advantages of storage phosphor or CR systems over conventional film-screen approaches include the potential for reduction of patient exposure and the virtual elimination of retakes due to improper technique. There is some advantage of the storage phosphor system over other digital radiographic techniques in that the storage phosphor plate simply replaces the screen/film cassette and does not represent a significant change in patient positioning or other imaging procedures and no need for specialized equipment or service personnel [Hendee et.al 2002]. Another advantage of digital radiography is that the image is available for computer post processing such as image enhancement and quantification. Moreover, the image can easily be stored and transported in digital form, making the images more accessible and making large film archives unnecessary. Today, digital picture archiving and communication systems (PACS) are part of hospital information systems, making the medical images immediately available through the digital network in the same way as the other patient information [P. Suetens 2009].

### **2.2.2 Direct Digital Radiography systems:**

Direct conversion requires a photoconductor that converts x-ray photons into electrical charges by setting electrons free [Yaffe et.al 1997]. Typical photoconductor materials include amorphous selenium, lead iodide, lead oxide, thallium bromide, and gadolinium compounds. The most commonly used element is selenium.

All of these elements have a high intrinsic spatial resolution [Zhao 1995]. As a result, the pixel size, matrix, and spatial resolution of direct conversion

detectors are not limited by the detector material itself, but only by the recording and readout devices used.

Selenium-based direct conversion DR systems are equipped with either a selenium drum or a flat-panel detector. In the former case, a rotating selenium-dotted drum, which has a positive electrical surface charge, is exposed to x-rays. During exposure, a charge pattern proportional to that of the incident x-rays is generated on the drum surface and is recorded during rotation by an analog-to-digital converter [Yaffe 1997]. Several clinical studies have confirmed that selenium drum detectors provide good image quality that is superior to that provided by screen-film or CR systems. However, because of their mechanical design, selenium drum detectors are dedicated thorax stand systems with no mobility at all.

A newer generation of direct conversion DR systems make use of selenium-based flat-panel detectors. These detectors make use of a layer of selenium with a corresponding underlying array of thin-film transistors (TFTs). Which material that will pass an electrical charge on irradiation. It is deposited on the amorphous silicon TFT array as a single layer of material. The upper surface is bonded to an electrode to a high positive potential [Allisy et.al 2008]. With direct detectors, the electrons released in the detector layer from x-ray interactions are used to form the image directly. Light photons from a scintillator are not used. A negative voltage is applied to a thin metallic layer (electrode) on the front surface of the detector, and therefore the detector elements are held positive in relation to the top electrode. During x-ray exposure, x-ray interactions in the selenium layer liberate electrons that migrate through the selenium matrix under the influence of the applied electric field and are collected on the detector elements. After exposure, the detector elements are read out as described earlier for indirect systems [Bushberg et.al 2002].

The TFT array corresponds to an array of pixels in the final image, with the number of transistors equalling the number of pixels. Flat-panel detectors having pixel sizes on the order of 200 micrometres (2.5 lp/mm resolution) are available for chest imaging, and a new generation of detectors with spatial resolution in the 50- to 100-micrometer (5- to 10-lp/mm) range is becoming available for mammography [Hendee et.al 2002]. An important feature of the newer generation of flat-panel detectors is their higher detective quantum efficiency (DQE). DQE is a measure of the detection efficiency that includes the effects of noise as well as resolution at various spatial frequencies. The DQE

of current flat-panel digital detectors is over 65%, while that of computed radiography storage phosphor systems is approximately 35%, and that of screen-film systems is approximately 25%. Because of the higher DQE, flat-panel detectors are expected to use radiation dose more efficiently, and they could theoretically provide lower noise images over the range of spatial frequencies encountered in medical imaging [P. Allisy et.al 2008].

### **2.2.3 Indirect Digital Radiography systems:**

In indirect conversion systems, a scintillation material converts the energy of the x-ray photons to visible light. Scintillation materials used for this purpose include amorphous silicon and cesium iodide [Hendee et.al 2002]. The term "indirect" comes from the fact that x-rays are absorbed in the screen, and the absorbed x-ray energy is then relayed to the photo detector by visible light photons. This indirect detection strategy is analogous to a screen-film system, except that the electronic sensor replaces the light-sensitive film emulsion. Dual-emulsion film is thin and x-rays penetrate it easily; therefore, in a screen-film cassette, the film is sandwiched between screens to reduce the average light propagation path length and improve spatial resolution. Flat panels are thicker than film and do not transmit x-rays well; consequently, a sandwiched design is not possible. Instead, the intensifying screen is layered on the front surface of the flat panel array. This means that the light emanating from the back of the intensifying screen strikes the flat panel, and much of the light that is released in the screen has to propagate relatively large distances through the screen, which results in more blurring. To improve this situation, most flat panel detector systems for general radiography use CsI screens instead of  $\text{Gd}_2\text{O}_2\text{S}$ . CsI is grown in columnar crystals, and the columns act as light pipes to reduce the lateral spread of light [Bushberg et.al 2002]. Photoconductors used in indirect conversion systems include CCDs and materials such as amorphous silicon coupled with a TFT array [Hendee et.al 2002].

The disadvantages of DR in comparison with CR or film-screen radiography are cost and versatility. A radiographic room generally has two Bucky position: in the table and in the chest stand. For DR, two separate (very expensive) detectors would be required, whereas a single CR reader will serve not only both Buckys but also additional X-ray rooms [P. Allisy et.al 2008].



## **2.3 Image Quality:**

### **2.3.1 Spatial Resolution:**

Spatial resolution refers to the minimum resolvable separation between high-contrast objects. In digital detectors, spatial resolution is defined and limited by the minimum pixel size. The image resolution of a radiographic system depends on several factors. The size of the focal spot. The anode tip should make a large angle with the electron beam to produce a nicely focused X-ray beam. Thicker patients cause more X-ray scattering, deteriorating the image resolution. Patient scatter can be reduced by placing a collimator grid in front of the screen. The grid allows only the photons with low incidence angle to reach the screen. The light scattering properties of the fluorescent screen. The film resolution, which is mainly determined by its grain size. For image intensifier systems and digital radiography, the sampling step at the end of the imaging chain is an important factor.

The resolving power (i.e., the frequency where the MTF is 10%) of clinical screen–film combinations varies from 5 up to 15 lp/mm. In most cases, spatial resolution is not a limiting factor in reader performance with film. For images with storage phosphors, a resolving power of 2.5 up to 5 lp/mm (at 10% contrast) is obtained. This corresponds to a pixel size of 200 to 100  $\mu\text{m}$ , which is mostly sufficient except for mammography, for which more recent detector technology is needed. Depending on the size of the object, it is clear that images with 2000 by 2000 pixels and even more are needed to obtain an acceptable resolution [Bushberg et.al 2002].

### **2.3.2 Contrast:**

The contrast is the intensity difference in adjacent regions of the image. Image intensity depends on the attenuation coefficients  $\mu(E, x)$  and thicknesses of the different tissue layers encountered along the projection line. Because the attenuation coefficient depends on the energy of the X-rays, the spectrum of the beam has an important influence on the contrast. Soft radiation yields a higher contrast than hard radiation. Another important factor that influences the contrast is the absorption efficiency of the detector, which is the fraction of the total radiation hitting the detector that is actually absorbed by it. A higher absorption efficiency yields a higher contrast. In systems with film, the contrast

is strongly determined by the contrast of the photographic film. The higher the contrast, the lower the useful exposure range. In digital radiography, contrast can be adapted after the image formation by using a suitable gray value transformation. Note however that such a transformation also influences the noise, thus keeping the CNR unchanged [Bushberg et.al 2002].

### **2.3.3 Noise:**

Quantum noise, which is due to the statistical nature of X-rays, is typically the dominant noise factor. A photon-detecting process is essentially a Poisson process (the variance is equal to the mean). Therefore, the noise amplitude (standard deviation) is proportional to the square root of the signal amplitude, and the SNR also behaves as the square root of the signal amplitude. This explains why the dose cannot be decreased unpunished. Doing so would reduce the SNR to an unacceptable level. Further conversions during the imaging process, such as photon–electron conversions, will add noise and further decrease the SNR.

To quantify the quality of an image detector the measure detective quantum efficiency (DQE) is often used. The image detector is one element in the imaging chain and to quantify its contribution to the SNR, the DQE is used, which expresses the signal-to-noise transfer through the detector. The DQE can be calculated by taking the ratio of the squared SNR at the detector output to the squared SNR of the input signal as a function of spatial frequency. It is a measure of how the available signal-to-noise ratio is degraded by the detector. Several factors influence the DQE, particularly the absorption efficiency of the detector, the point spread function of the detector and the noise introduced by the detector [Bushberg et.al 2002].

### **2.3.4 Artifacts:**

Although other modalities suffer more from severe artifacts than radiography, X-ray images are generally not artifact free. Scratches in the detector, dead pixels, unread scan lines, inhomogeneous X-ray beam intensity (heel effect), afterglow, etc., are not uncommon and deteriorate the image quality [Bushberg et.al 2002].

### **2.3.5 Modulation Transfer Function:**

Modulation transfer function (MTF) is the capacity of the detector to transfer the modulation of the input signal at a given spatial frequency to its output [Spahn 2005]. At radiography, objects having different sizes and opacity are displayed with different gray-scale values in an image. MTF has to do with the display of contrast and object size. More specifically, MTF is responsible for converting contrast values of different-sized objects (object contrast) into contrast intensity levels in the image (image contrast). For general imaging, the relevant details are in a range between 0 and 2 cycles/mm, which demands high MTF values.

MTF is a useful measure of true or effective resolution, since it accounts for the amount of blur and contrast over a range of spatial frequencies. MTF values of various detectors were measured and further discussed by Illers et.al [Illers et.al 2005].

### **2.3.6 Dynamic Range:**

Dynamic range is a measure of the signal response of a detector that is exposed to x-rays. In conventional screen-film combinations, the dynamic range gradation curve is S shaped within a narrow exposure range for optimal film blackening thus, the film has a low tolerance for an exposure that is higher or lower than required, resulting in failed exposures or insufficient image quality. For digital detectors, dynamic range is the range of x-ray exposure over which a meaningful image can be obtained. Digital detectors have a wider and linear dynamic range, which, in clinical practice, virtually eliminates the risk of a failed exposure. Another positive effect of a wide dynamic range is that differences between specific tissue absorptions (e.g. bone vs soft tissue) can be displayed in one image without the need for additional images. On the other hand, because detector function improves as radiation exposure increases, special care has to be taken not to overexpose the patient by applying more radiation than is needed for a diagnostically sufficient image [Spahn 2005].

### **2.3.7 Detective Quantum Efficiency:**

Detective quantum efficiency (DQE) is one of the fundamental physical variables related to image quality in radiography and refers to the efficiency of a detector in converting incident x-ray energy into an image signal. DQE is calculated by comparing the signal-to-noise ratio at the detector output with that at the detector input as a function of spatial frequency [Spahn 2005]. DQE is dependent on radiation exposure, spatial frequency, MTF, and detector material. The quality (voltage and current) of the radiation applied is also an important influence on DQE [Illers et.al 2005].

High DQE values indicate that less radiation is needed to achieve identical image quality; increasing the DQE and leaving radiation exposure constant will improve image quality.

The ideal detector would have a DQE of 1, meaning that all the radiation energy is absorbed and converted into image information. In practice, the DQE of digital detectors is limited to about 0.45 at 0.5 cycles/mm. During the past few years, various methods of measuring DQE have been established [Illers et.al 2005]. Making the comparison of DQE values difficult if not impossible. In 2003, the IEC62220–1 standard was introduced to standardize DQE measurements and make them comparable.

## **2.4 Radiation Protection:**

### **2.4.1 Biological Effect of Ionizing Radiation:**

Most adverse health effects of radiation exposure may be grouped in two general categories: Deterministic effects and stochastic effect.

#### **2.4.1.1 Deterministic Effects:**

These include the type of injuries resulting from whole body or local exposure to radiation that causes sufficient cell damage or cell killing to substantial numbers or proportion of cells to impair functions in the irradiated tissues or organs. A certain threshold has to be exceeded before the effect is seen , and above the threshold , the severity of the effect is dose related i.e. it will increase with increasing dose rate .The doses that result in the clinical appearance of the

deterministic effects are generally of the order of few Gray (Gy ) to tens of Gray .The time at which the effect becomes noticeable may extend from a few hours to some years after exposure , depending on the type of effect and type of the irradiated tissues [ICRP 1977].

#### **2.4.1.2 Stochastic Effects:**

Instead of being killed, the irradiated cell may be modified and continue to reproduce, potentially causing malignancy. Unlike the deterministic effects, there is no threshold for stochastic effect to occur. The probability of an effect occurring is a function of dose, but the severity of the effect is dose independent [ICRP 1977]. Stochastic effects can be categorized as somatic (carcinogenic) effects or hereditary (genetic) effects, which may occur from injury to one or a small number of cells. Since a single cell may be enough to initiate the effect, there is a finite probability that the effect will occur however small the dose [ICRP 1977].

#### **2.4.2 System of Radiological Protection:**

The international commission on radiological protection (ICRP) has formulated the system of radiological protection of the human from harmful effect of ionizing radiation. This system is based on three principles: Justification, optimization and dose limit.

##### **2.4.2.1 Justification:**

No practice or source within a practice should be authorized unless the practice produces sufficient benefit to the exposed individuals or to society to offset the radiation harm that it might cause; that is: unless the practice is justified, taking into account social, economic and other relevant factors [IAEA 1996].

##### **2.4.2.2 Optimization:**

In relation to any particular source within a practice , the magnitude of individual doses , the number of people exposed , and the likelihood of exposure , where they are not certain to be received , should all be kept as low as reasonably achievable (ALARA), with economic and social factors being taken into account [IAEA 1996].

### **2.4.2.3 Dose limit:**

The exposure of individuals resulting from the combination of all the relevant practices should be subject to dose limits. These are aimed at ensuring that no individual exposed to radiation risks from such practices which are judged to be unacceptable in any normal circumstances. Not all sources of radiation are susceptible to control by action at the facility, and it is necessary to specify the sources to be included as relevant before selecting a dose limit. For medical purpose, dose limits are not applied. If a practice is justified and protection optimized, the dose to patient will be as low as compatible with the medical procedure. Any further constraint of doses might lead to the patient's detriment [IAEA 1996].

## **2.5 Dose measurement methodology:**

### **2.5.1 Determination of ESD from TLD measurement:**

TLD are considered as the gold standard for determination of entrance surface dose in practice. Measurement is made with thermo-lumen since dosimeter, TLDs attached to the patient or phantom at pointes where the X-ray beam enters the patient. TLDs are read in a standard manner and the value read is used as an estimate of the ESD received by the patient. If correctly calibrated to measure air kerma free in air, the TLD should give a direct reading of the entrance surface dose, and no correction is needed for back scatter radiation or distance from the tube focus.

### **2.5.2 Calculation of ESD from tube output data:**

ESD may be calculated in practice by means of knowledge of tube output. the relationship between x-ray unit current time product (mAs) and the air kerma free in air is establish at reference point in the x-ray field at 80 kVp tube potential . Subsequent estimate of the ESAK can be done by recording the relevant parameters (tube potential, filtration, mAs and FSD) and correcting for distance and backscatter radiation according to the following equation:

$$\text{ESD} = \text{OP} \times \left[\frac{\text{kv}}{80}\right]^2 \times \text{mAs} \times \left[\frac{100}{\text{FSD}}\right]^2 \times \text{BSF} \quad \rightarrow (2 - 1)$$

Where OP is the tube output per mAs measured at a distance of 100 cm from the tube focus along the beam axis at 80 kVp, kVp is peak tube voltage recorded for any given examination, mA s is the tube current–time product, FSD is the focus-to- patient entrance surface distance and BSF is the backscatter factor [Toivonen 2001].

## **2.6 Previous study:**

### **2.6.1 Suliman et.al (2007) Entrance surface doses to patients undergoing selected diagnostic X-ray examinations in Sudan:**

The aim of the authors in that study was to evaluate the entrance surface doses (ESDs) to patients undergoing selected diagnostic X-ray examinations in major Sudanese hospitals. That work was carried out in four major hospitals in the Sudanese capital Khartoum. Eight X-ray units were included in the study. ESD per examination was estimated from X-ray tube output parameters in four hospitals comprising eight X-ray units and a sample of 346 radiographs. The hospitals that participated in the study were Ribat University Hospital (RUH), Khartoum Teaching Hospital (KTH), Omdurman Teaching Hospital (OTH) and Khartoum North Teaching Hospital (KNTH).

Hospital mean ESDs estimated range from 0.17 to 0.27 mGy for chest AP, 1.04–2.26 mGy for Skull AP/PA, 0.83–1.32 mGy for Skull LAT, 1.31–1.89 mGy for Pelvis AP, 1.46–3.33 mGy for Lumbar Spine AP and 2.9–9.9 mGy for Lumbar Spine LAT. With exception of chest PA examination at two hospitals, mean ESDs were found to be within the established international reference doses.

### **2.6.2 Suleiman A et.al (2014) Assessment of Entrance Surface Dose for the Patients from Common Radiology Examinations in Sudan:**

In this study, Entrance Surface dose (ESD) were estimated for adults patients undergoing common X- ray examinations in two Hospitals in Khartoum, namely Khartoum teaching hospital and academy teaching hospital. The study was performed in four X-ray machines. A total of 191 patients were included in this study. Patient's data such as (age and weight) and exposure parameters (kV and mAs) were recorded. The results of ESD have been obtained with the use of the Dose Cal software which developed by the radiological protection center in

saint gorges hospital London. The results showed that the mean values for chest, abdomen and limbs were 0.31 mGy, 2.6 mGy, 0.05 mGy respectively. The results obtained in this work, range from

(10.3) for lumbosacral lat to (0.004) for Elbow, was not exceeding the reference value and also the values obtained by previous studies. But when comparison made between the four machines using some selected tests, the mean dose value at Khartoum teaching hospital by (shimadzu (1)) was found to be higher than other machines. This may be due the fact that the machine is old one and also its output is greater than outputs of other machines, but in general the competency of technicians in Khartoum teaching hospital is less than in the academy teaching hospital, and also the number of patients in this hospital is more than academy hospital.

### **2.6.3 H. Osman et.al (2013) Assessment of Paediatric Radiation Dose from Routine X-Ray Examination: A**

#### **Hospital Based Study, Taif Paediatric Hospital:**

The main aim of the current study was to determine Entrance Surface Dose (ESD) to paediatric patients as the result of imaging procedure, in main paediatric hospital in Taif city –Saudi Arabia for the first time. 110 patients underwent different examinations (chest, abdomen, skull, and extremities), age range from 0-15 years. The patients bio data (age, weight, height, gender) were recorded. The exposure factors, focal skin distance, tube output and back scatter factor were entered in special software known by DOS CAL in order calculate the ESDs. The mean ESD obtained ranged 0.18 -0.32 mGy per radiograph for different ages and groups. The results for paediatric radiation dose were agreed and compatible with literature.

### **2.6.4 A.K. Sam et.al (2010) Radiation Dose Measurements in Routine X ray Examinations:**

The aim of current study was to evaluate patient's radiation dose in routine X-ray examinations in Omdurman teaching hospital Sudan. 110 patients was examined (134) radiographs in two X-ray rooms. Entrance surface doses (ESDs) were calculated from patient exposure parameters using DosCal software. The mean ESD for the chest, AP abdomen, AP pelvis, thoracic spine AP, lateral lumbar spine, anteroposterior lumbar spine, lower limb and for the



upper limb were;  $231 \pm 44 \mu\text{Gy}$ ,  $453 \pm 29 \mu\text{Gy}$ ,  $567 \pm 22 \mu\text{Gy}$ ,  $311 \pm 33 \mu\text{Gy}$ ,  $716 \pm 39 \mu\text{Gy}$ ,  $611 \pm 55 \mu\text{Gy}$ ,  $311 \pm 23 \mu\text{Gy}$ , and  $158 \pm 57 \mu\text{Gy}$ , respectively. Data shows asymmetry in distribution. The results of were comparable with previous study in Sudan.

## **Chapter three**

### **Material and Methods**

#### **3.1 Material:**

##### **3.1.1 Study sampling:**

In this study the data were collected from 54 patients, who underwent routine x-ray examinations for (chest, pelvis, lumbar spine, cervical spine, lower limb and the upper limb) with digital imaging in the x-ray department of modern medical centre in Khartoum state.

##### **3.1.2 Machine use:**

The x-ray machine used in this study was Toshiba manufactured june2013, unit model E7242X, max voltage 125kv, focal spot 1.5/0.6.

#### **3.2 Methods:**

For each patient, the age, weight, height, body mass index (BMI), and exposure parameters: peak tube voltage (kVp), exposure current– time product (mAs) and focus-to-film distance (FFD) were recorded.

The ESD was calculated using the following relation:

$$\text{ESD} = \text{OP} \times \left[\frac{\text{kV}}{80}\right]^2 \times \text{mAs} \times \left[\frac{100}{\text{FSD}}\right]^2 \times \text{BSF} \rightarrow (3 - 1)$$

Where (OP) is the tube output per mAs measured at a distance of 100 cm from the tube focus along the beam axis, kV is peak tube voltage recorded for any given examination, mAs is the tube current and time product, FSD is the focus-to-patient entrance surface distance and BSF is the backscatter factor, with a value of 1.35 in this study.

The kV and mAs was changed according to the type of examination and patient age, height and Weight. The ESD was used to assess radiation dose to the patient for the following selected examinations: chest, lumbar spine AP, lumbar spine LAT, cervical spine AP, cervical spine LAT, pelvis AP, lower limb and the upper limb. This ensured that all dose levels used were representative of the diagnostic image. The results were picked up with different figures, tables, groups and graphs using excel software of windows Microsoft and correlation was found between BMI and ESD.

## Chapter four

### Results

The following tables and figures represent the data obtained from 54 patients underwent routine x-ray examinations for (chest, pelvis, lumber spine, cervical spine, lower limb and the upper limb) with digital imaging in the x-ray department of modern medical centre in Khartoum state.

**Table 4-1: The gender distribution frequency and percentages.**

Gender	Frequency	Percentages
Male	28	51.85%
Female	26	48.15%

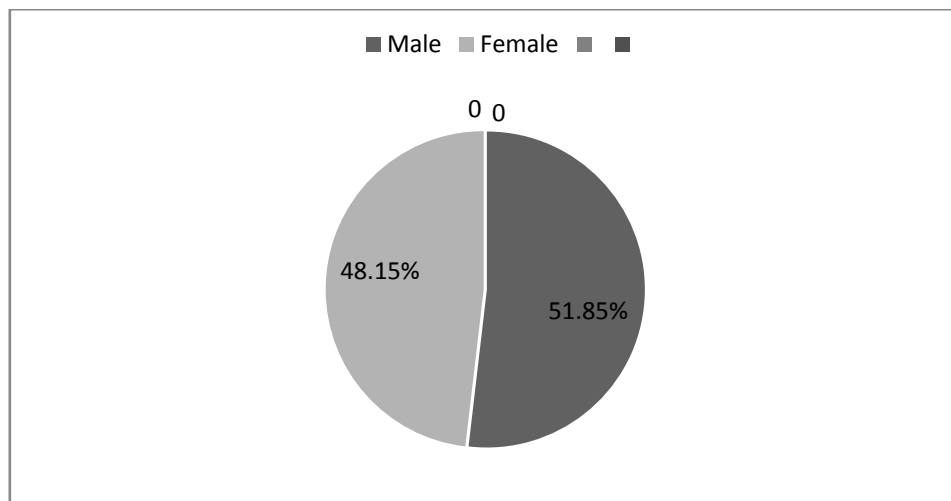


**Figure 4-1: The gender distribution percentages.**

**Table 4-2: Statistical summary ESDs and exposure parameters for selected x-ray examination.**

<b>Examination</b>	<b>kVp</b>	<b>mAs</b>	<b>FFD(cm)</b>	<b>ESD(mGy)</b>
<b>chest</b>	116-120	3.2-8	180	0.25±0.07
<b>Upper limb AP</b>	48-60	3.2-16	100	0.28±0.25
<b>Upper limb LAT</b>	50-62	3.2-12.5	100	0.2±0.17
<b>Cervical spine AP</b>	63-120	4-8	180	0.18±0.07
<b>Cervical spine LAT</b>	63-120	4-8	180	0.18±0.07
<b>Lumber spine AP</b>	70-76	25-40	100	1.8±0.3
<b>Lumber spine LAT</b>	79-88	25-50	100	2.89±0.7
<b>Pelvis</b>	69-79	16-25	100	1.26±0.4
<b>Lower limb AP</b>	48-70	4-12.8	100	0.2±0.07
<b>Lower limb LAT</b>	50-68	8-10.2	100	0.38±0.15

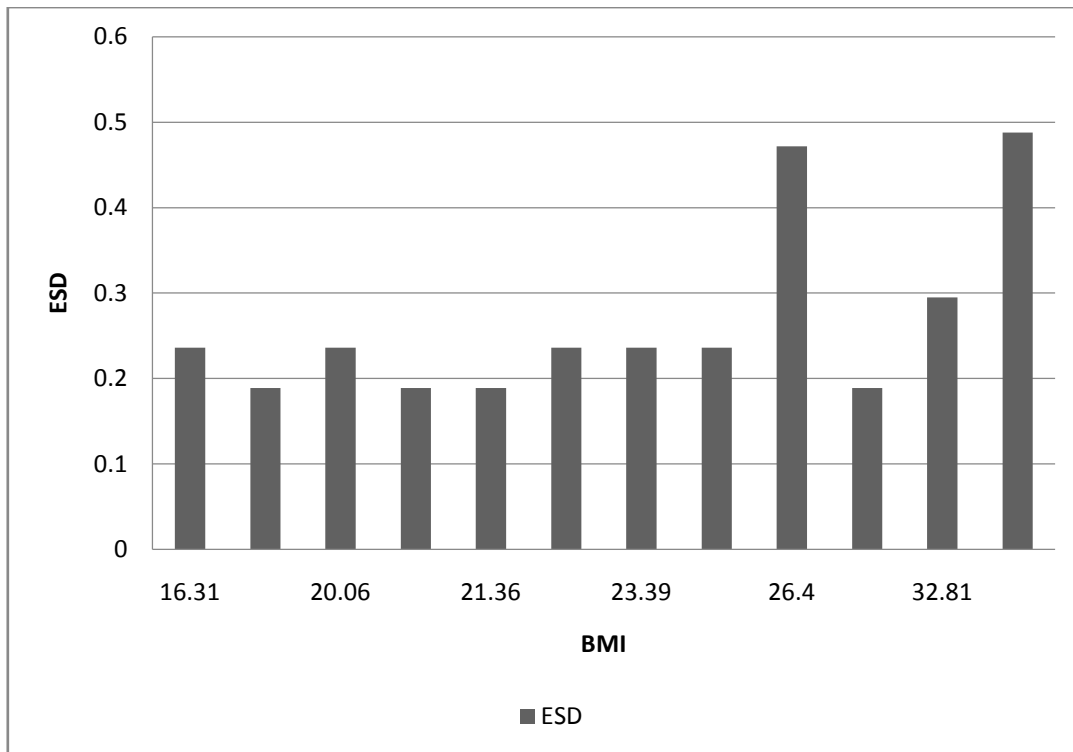


**Figure 4-2: The correlation between ESD (mGy) BMI (Kg/m<sup>2</sup>) of patients undergoing chest X-ray.**

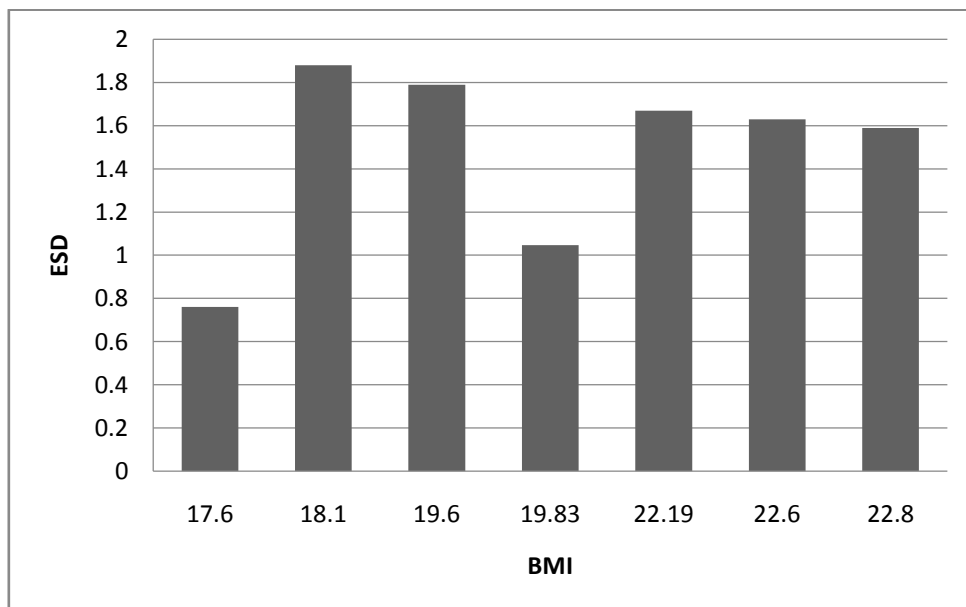


**Figure 4-3: The correlation between ESD and BMI of patients undergoing L/S and pelvis x-ray.**

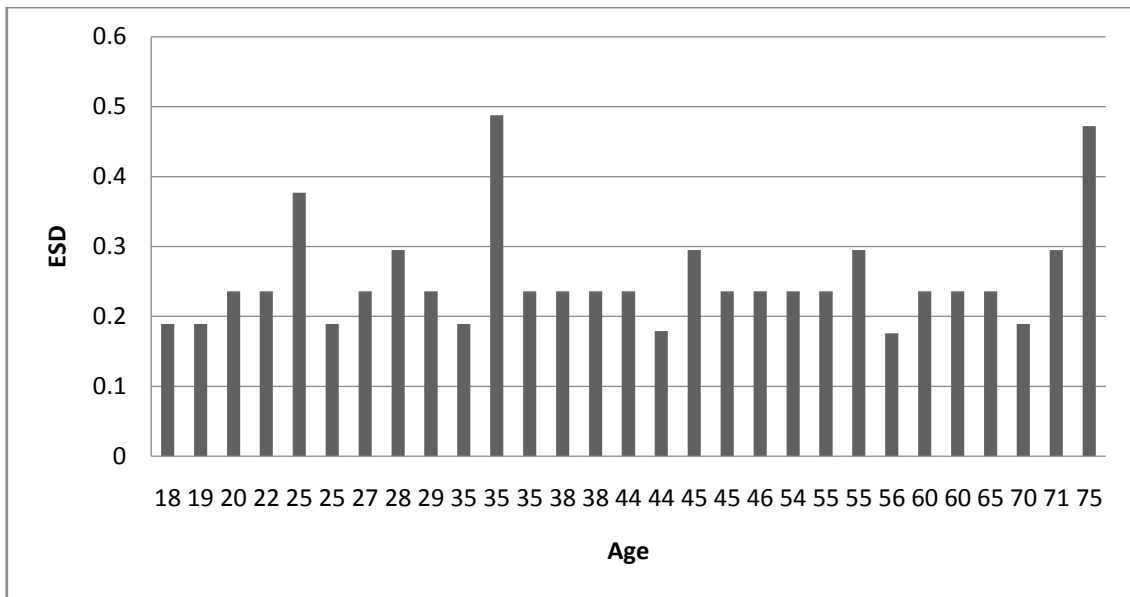


**Figure 4-4: The correlation between ESD (mGy) and Age for chest x-ray.**

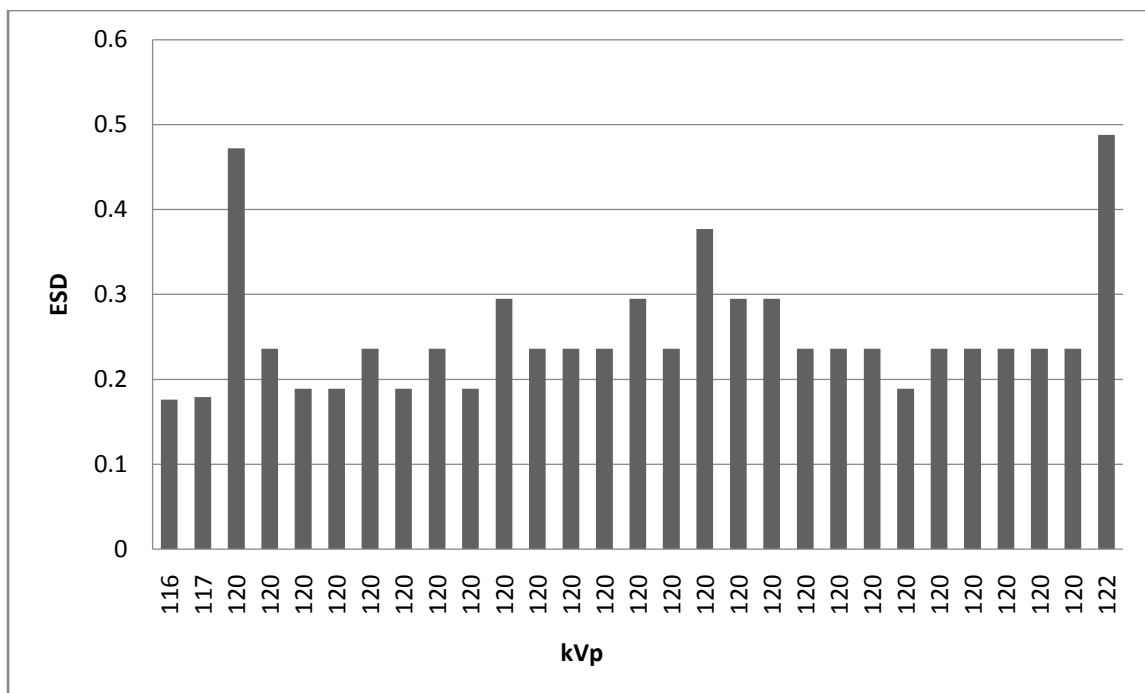
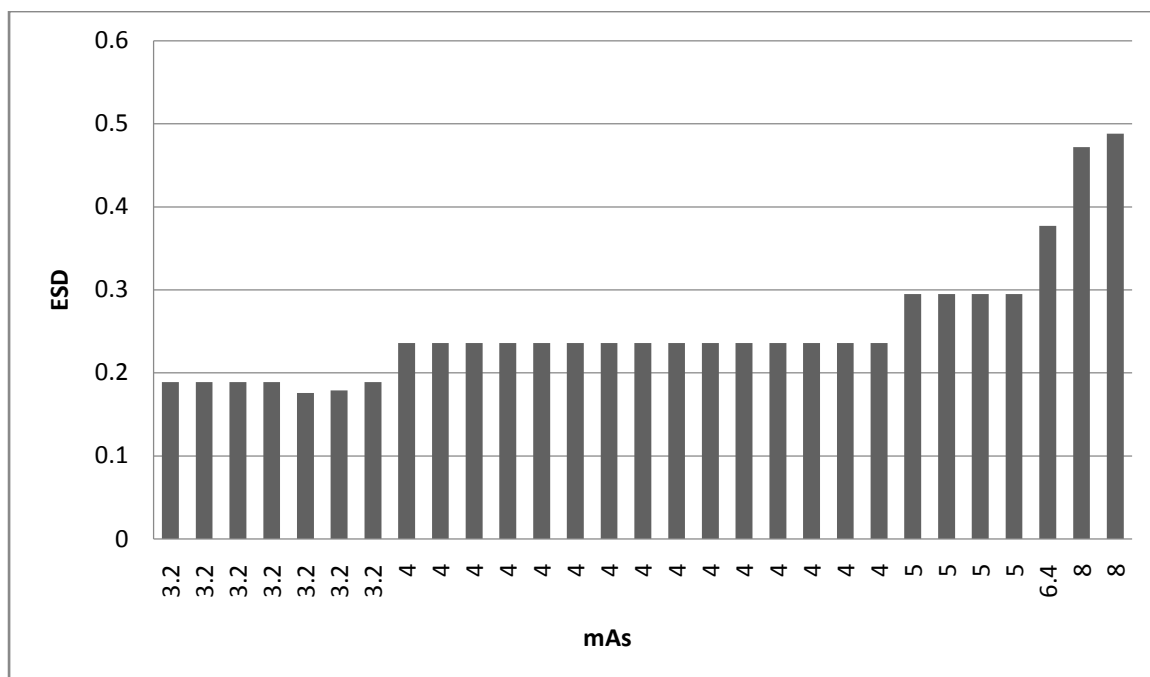


**Figure 4-5: The correlation between ESD (mGy) and kVp for chest x-ray.**





## Chapter five

### Discussions, Conclusion and Recommendations

#### 5.1 Discussions:

This study intended to estimate the radiation entrance skin doses for patients undergoing some diagnostic x-ray examinations by digital radiography. It was anticipated that the study would help in the optimization of radiation protection of the patient. The data were collected from in Modern Medical Centre in Khartoum.

The findings of this study was that the mean ESD for the chest PA, Upper limb AP, Upper limb LAT, Cervical spine AP, Cervical spine LAT, lumbar spine AP, lumbar spine LAT, pelvis, lower limb AP and for lower limb LAT. were;  $0.25 \pm 0.07 \text{mGy}$ ,  $0.28 \pm 0.25 \text{mGy}$ ,  $0.2 \pm 0.17 \text{mGy}$ ,  $0.18 \pm 0.07 \text{mGy}$ ,  $0.18 \pm 0.07 \text{mGy}$ ,  $1.8 \pm 0.3 \text{mGy}$ ,  $2.89 \pm 0.7 \text{mGy}$ ,  $1.26 \pm 0.4 \text{mGy}$ ,  $0.2 \pm 0.07 \text{mGy}$  and  $0.38 \pm 0.15 \text{mGy}$  respectively.

When comparing this findings ESD values with reference levels and with previous studies in Sudan and other countries, the mean ESDs relatively less than previous studies and reference because the machine is high sensitive than other (Table 4.2).

The other findings of this study there is no correlation found between ESD and age, but there significant correlation between ESD and BMI, because the exposure parameters depend on the size of patients and type of examinations not the age.

From the results, using of digital image machines is better because the output of tube is low and so patients will be given low dose, and no need to give high kV to obtained good images.

## **5.2 Conclusion:**

ESDs were estimated in the present study for patients underwent selected diagnostic X-ray examinations with digital imaging in the x-ray department of Modern Medical Centre in Khartoum, the mean ESDs relatively less than previous studies in Sudan or other countries and reference. No correlation was found between ESD and Age but significant correlation between ESD and body mass index.

### **5.3 recommendation:**

- Increase the technologist's training to guidelines for quality radiograph for standardizing their practice and as to avoid repeating the dose for patients.
- Replace all conventional x-rays by the digital radiography.
- Further studies are required in order to optimize radiation dose and establish local diagnostic reference level DRL.

## References:

- Antonuk L. E, Yorkston J, Huang W, et al. A real-time, flat-panel, amorphous silicon, digital x-ray imager. *RadioGraphics* 1995.
- Choquette M, Demers Y, Shukri Z, et al. Performance of a real-time selenium-based x-ray detector for fluoroscopy. *Proc SPIE* 2001.
- Colbeth R, Boyce S, Fong R, et al. 40 × 30 cm flat-panel imager for angiography, R&F, and cone-beam CT applications. *Proc SPIE* 2001.
- Davidson RA. Radiographic contrast-enhancement masks in digital radiography. [PhD Thesis] New South Wales, Australia: The University of Sydney; 2006.
- Gallet J, Van Metter R. Image capture chain performance of Kodak's next generation of DIRECTVIEW DR Systems (Kodak Medical Systems white paper) [Online] Available at <http://www.carestreamhealth.com/awp-dr.html>. (Accessed 3 September 2009).
- ICRP (1977) Publication 26; *Annals of the ICRP* 1(3). Recommendations of the International Commission on Radiological Protection, Pergamon Press, Oxford, England.
- Illers H, Buhr E, Gunther-Kohfahl S, et al. Measurement of the modulation transfer function of digital X-ray detectors with an opaque edge-test device. *Radiat Prot Dosimetry* 2005.
- International Atomic Energy Agency. International basic safety standards for protection against ionizing radiation and for the safety of radiation sources. (1996). IAEA Safety Series no. 115 (Vienna: IAEA).
- J. T. Bushberg, J. A. Seibert, E. M. Leidholdt, J. M. Boone (2002) *The Essential Physics of Imaging*, 2<sup>nd</sup> edn.
- Kandarakis I, Cavouras D, Panayiotakis G. S, et al. Evaluating x-ray detectors for radiographic applications: a comparison of ZnSCdS:Ag with Gd<sub>2</sub>O<sub>2</sub>S:Tb and Y<sub>2</sub>O<sub>2</sub>S:Tb screens. *Phys Med Biol* 1997.
- Kruger R. A, Mistretta C. A, Crummy A. B, et al. Digital K-edge subtraction radiography. *Radiology* 1977.
- Marshall NW. An examination of automatic exposure control regimes for two digital radiography systems. *Phys Med Biol*. 2009; 154(15):4645–70. [PubMed].
- Moore R. Computed radiography. *Med Electron* 1980.

- Neitzel U, Maack I, Gunther-Kohfahl S. Image quality of a digital chest radiography system based on a selenium detector. *Med Phys* 1994.
- Ovitt T. W, Christenson P. C, Fisher H. D 3rd, et al. Intravenous angiography using digital video subtraction: x-ray imaging system. *AJR Am J Roentgenol* 1980.
- P. Allisy, R. J. Williams (2008) *Farr's Physics for Medical Imaging* 2<sup>nd</sup> edn. Philadelphia.
- P. Suetens (2009) *Fundamentals of Medical Imaging* 2<sup>nd</sup> edn. Cambridge University.
- Puig S. Digital radiography of the chest in pediatric patients [in German]. *Radiologe* 2003.
- Schaefer-Prokop C, De Boo D, Uffmann M, et al. DR and CR: Recent advances in technology. *Eur J Radiol.* 2009 (in press). [PubMed].
- Spahn M. Flat detectors and their clinical applications. *Eur Radiol* 2005.
- Toivonen M, (2001) Patient dosimetry protocol in digital and interventional radiology *Radiat. Port. Dosim.* 94,1-2,105-8.
- W. R. Hendee, E. R. Ritenour (2002) *Medical Imaging Physics* 4<sup>th</sup> edn. New York.
- Yaffe M. J, Rowlands J. A. X-ray detectors for digital radiography. *Phys Med Biol* 1997.
- Zhao W, Rowlands J. A. X-ray imaging using amorphous selenium: feasibility of a flat panel self-scanned detector for digital radiology.